Semi-Analytical Formulation for the Phase-Noise Analysis of Injection-Locked Push-Push Oscillators

Elena Fernández, Mabel Pontón, Franco Ramírez, Sergio Sancho, Almudena Suárez

DICOM, Universidad de Cantabria
39005 Santander, Spain
ramirezf@unican.es

***Abstract*— This paper presents a semi-analytical formulation for the phase-noise analysis of injection-locked push-push oscillators. The formulation provides insight into the noise spectrum and its corner frequencies, which can be related to some design parameters. It enables a direct comparison with the phase-noise spectrum of a single injection-locked oscillator, based on one of the two sub-oscillator circuits. The push-push configuration is optimized in order to increase the synchronization bandwidth and the phase-noise spectrum before and after this optimization is compared. The formulation, applied to 10.4 GHz oscillator, has been validated with the accurate conversion matrix approach and with experimental measurements.**

I. Introduction

Push-push oscillators allow increasing the frequency generation capabilities of microwave devices. In push-push oscillators, two individual oscillators, with 180º phase shift at the fundamental frequency f_0, are combined to produce an output at $2f_0$, through the cancellation of the odd harmonic terms [1]. The even harmonic terms are added in phase so we obtain a 3 dB power increase with respect to the individual oscillator. When injection-locked at the fundamental frequency, it basically operates as a frequency doubler, requiring only a very small input power and still providing an inherent cancellation of odd harmonic terms [2]. The low input power is due to the fact that the oscillator is operating as fundamentally synchronized oscillator, which typically requires very small power from the input source. In injection-locked mode, the output phase noise will approximately double the one corresponding to the input source up to a certain offset frequency and then it will approach the phase noise of the free-running push-push at $2f_0$. Thus, it would be interesting to be able to identify the circuit magnitudes or parameters that determine this change of behavior. The injection-locked push-push oscillator can be applied as a frequency doubler when only a small power source at f_0 is available. Attention must also be paid to the synchronization bandwidth to guarantee a robust behavior versus temperature changes or component tolerances.

Previous works have presented analytical expressions for the estimation of the phase-noise spectrum of an injection-locked push-push oscillator. However, the expressions, based on Adler's formulation for the analysis of injection-locked oscillators, turn out to be too simplified to accurately predict the phase-noise behavior when using transistor devices. In this paper, we use a semi-analytical formulation for the in-depth and realistic study of the phase-noise spectrum. The formulation extends the one presented in [3] (applied to a single oscillator circuit) to the case of push-push oscillators. The results will be compared with the accurate conversion-matrix approach, implemented on harmonic balance (HB). The advantage of the semi-analytical formulation is that provides more insight into the magnitudes that determine the shape of the noise spectrum. The behavior of two different push-push designs at 10 GHz, with different locking bandwidth, will be compared with that of a single sub-oscillator circuit.

II. Injection-locked Push-push Oscillator

The free-running push-push oscillator is composed of two individual oscillator circuits with 180º phase shift. Thus, for the injection-locking we use a rat-race coupler, as depicted in Fig. 1. The used active device is a bipolar transistor (BFP405) and the circuit has been manufactured on CuClad 2.17 substrate ($h = 0.254$ mm). The outputs of the oscillators are combined through a Wilkinson power combiner. The base and collector bias voltages (V_{bb} and V_{cc}, respectively) are set to 5 V. The circuit oscillates at 5.2 GHz and the output frequency is 10.4 GHz. In order to preserve the circuit symmetry, one of the transistors has been back-mounted.

The push-push oscillator will operate as a fundamentally synchronized oscillator, with input frequency ω_s in the neighborhood of ω_0 and output frequency $2\omega_s$. Initially the circuit is analyzed in HB. For that, we make use of two auxiliary generators (AGs) at the fundamental frequency $\omega_{AG} = \omega_s$. The objective is to avoid non-oscillatory solutions at any of the two sub-oscillator circuits. The AG is a voltage generator, with amplitude A_{AG} and phase ϕ_{AG}, with an ideal bandpass filter at ω_{AG} . It must fulfill a non-perturbation condition of the oscillatory regime, given by the zero value of the current-to-voltage ratio $Y_{AG}=I_{AG}/A_{AG}$, with I_{AG} the current through the AG. The two AGs are connected symmetrically to equivalent nodes in the two subcircuits. We set the phase origin at the node of one of these two AGs, doing $\phi_{AG1}=0º$. Then, the second AG will have the phase value $\phi_{AG2}=180º$, which ensures the desired operation with 180º phase shift. For each value of input power and frequency, the two AGs must fulfill a non-perturbation condition given by:

$$\begin{aligned} &Y^1\left[V_1, V_2, \phi_1, \phi_2, \phi_g, j\omega_s\right]V_0 e^{j\phi_1} = 0, \quad \phi_1 = 0 \\ &Y^2\left[V_1, V_2, \phi_1, \phi_2, \phi_g, j\omega_s\right]V_0 e^{j\phi_2} = 0, \quad \phi_2 = \pi \end{aligned} \qquad (1)$$

The above equation is solved through optimization in commercial HB. The pure HB system constitutes the inner tier. For each input power and frequency, the variables to determine are the amplitudes V_1 and V_2 and the phase ϕ_{AG}. Note that due to the inherent symmetry of the push-push configuration the relationship $V_1=V_2$ is fulfilled. On the other hand, the synchronization bandwidth is obtained by sweeping the input-generator phase ϕ_g, calculating the AG amplitude A_{AG} and frequency ω_s at each sweep step. The synchronization curve for P_{in}=-26 dBm has been traced in terms of the output power at $2\omega_s$ in Fig. 2. The bandwidth of this original design is 2 MHz. The upper section of the ellipsoidal curve is stable and the lower section is unstable. Following the stability analysis techniques for N-push oscillators presented in [4],[5], we have also verified that the circuit does not exhibit any stable in-phase mode.

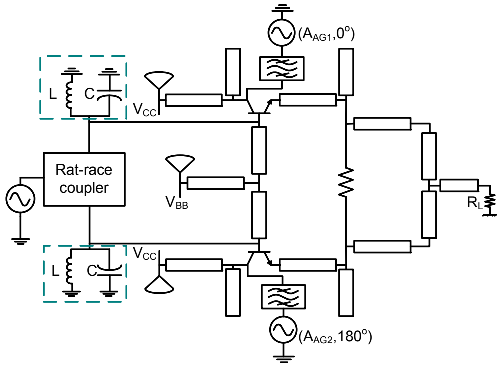

Fig. 1 Schematic of the injection-locked push-push oscillator. The injection signal is directly applied to the bases of the bipolar transistors using a rat-race coupler and a single external generator.

With the aim to increase the synchronization bandwidth, we have performed a second design, improving the input network. For that, we impose the synchronization condition at two frequency values ω_{s1},ω_{s2} with sufficient spacing $\Delta\omega_s=\omega_{s2}-\omega_{s1}$. At each frequency $\omega_{si}, i=1,2$ we solve (1) in terms of $V_1=V_2=V$, ϕ_g and an ideal reactive element (a capacitor in this case). After convergence at each of the two frequencies $\omega_{si}, i=1,2$ (in two different HB simulations) we obtain two ideal capacitance values ω_{s1}, C_1 and ω_{s2}, C_2. The impedance exhibited by these ideal capacitors at $\omega_{si}, i=1,2$ is implemented with a single reactive network using impedance synthesis techniques, in similar manner to the empirical technique for VCO linearization presented in [6],[7]. The synchronization bandwidth obtained with the modified input network can be compared with the original one in Fig. 2. This bandwidth has increases from 2 MHz to 12 MHz. Stable solutions correspond to the upper section of the curve. The modified circuit does not exhibit any stable in-phase mode.

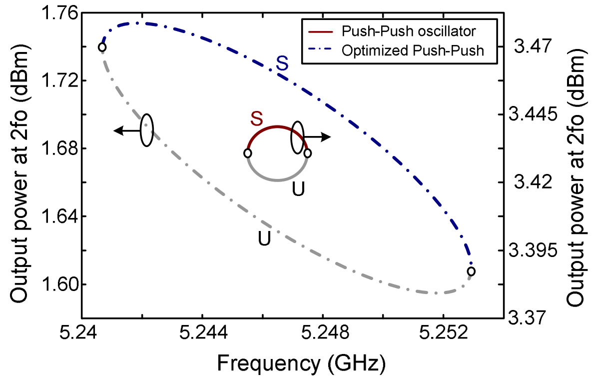

Fig. 2 Comparison of synchronization curves of the two different push-push oscillators. The upper sections of the curves are stable (S).

III. Semi-Analytical Formulation for Phase-Noise Analysis

To obtain a semi-analytical formulation for the prediction of the phase-noise spectrum we will perform a perturbation analysis of system (1). We will assume two types of noise perturbations: the phase noise $\psi(t)$ of the input generator and the white noise from the circuit itself, which is modeled with two equivalent white noise sources $I_{N1}(t)$ and $I_{N2}(t)$, at each of the two nodes considered in (1). In the presence of these perturbations, the phase and amplitude variables in (1) will be expressed as:

$$\begin{aligned}
&\phi_1 \to \phi_1+\psi(t)+\Delta\phi_1(t),\\
&\phi_2 \to \phi_2+\psi(t)+\Delta\phi_2(t),\\
&\phi_g \to \phi_g+\psi(t)\ ,\\
&V_1 \to V_0+\Delta V_1(t),\ \ V_2 \to V_0+\Delta V_2(t)\\
&j\omega_s \to j\omega_s+p
\end{aligned} \tag{2}$$

where p is a time-derivative operator. Next we will perform a Taylor series of the two admittance functions in (1) about a particular synchronized solution, defined by $V_1=V_2=V_0, \phi_{g0}, \omega_{s0}$. Note that, in spite of the symmetry relationships, the amplitude and phase perturbations will be different for the two sub-oscillators. Taking into account the action of the derivative operator p, we obtain the following system of linear differential equations:

$$\begin{aligned}
&\begin{bmatrix} Y^{1r}_{\phi_1} & Y^{1r}_{\phi_2} & Y^{1r}_{V_1} & Y^{1r}_{V_2}\\ Y^{1i}_{\phi_1} & Y^{1i}_{\phi_2} & Y^{1i}_{V_1} & Y^{1i}_{V_2}\\ Y^{2r}_{\phi_1} & Y^{2r}_{\phi_2} & Y^{2r}_{V_1} & Y^{2r}_{V_2}\\ Y^{2i}_{\phi_1} & Y^{2i}_{\phi_2} & Y^{2i}_{V_1} & Y^{2i}_{V_2} \end{bmatrix}\begin{bmatrix}\Delta\phi_1(t)\\ \Delta\phi_2(t)\\ \Delta V_1(t)\\ \Delta V_2(t)\end{bmatrix}+\begin{bmatrix} Y^{1r}_{\omega} & 0\\ Y^{1i}_{\omega} & 0\\ 0 & Y^{2r}_{\omega}\\ 0 & Y^{2i}_{\omega}\end{bmatrix}\begin{bmatrix}\Delta\dot{\phi}_1(t)\\ \Delta\dot{\phi}_2(t)\end{bmatrix}=\\
&=\frac{1}{V_0}\begin{bmatrix} I^r_{N1}(t)\\ I^i_{N1}(t)\\ I^r_{N2}(t)\\ I^i_{N2}(t)\end{bmatrix}-\dot{\psi}(t)\begin{bmatrix} Y^{1r}_{\omega}\\ Y^{1i}_{\omega}\\ Y^{1r}_{\omega}\\ Y^{1i}_{\omega}\end{bmatrix}
\end{aligned} \tag{3}$$

The matrixes in (3) are composed by the derivatives of the admittance functions in (1), with respect to the phases ϕ_1, ϕ_2, amplitudes V_1, V_2 and frequency ω_s. The subindex indicates the derivation variable and the superindexes r and i indicate real and imaginary parts. The derivatives are calculated through finite differences in HB. Small increments are applied to the two AGs used for the determination of the steady state solution in (1), as in the previous works [8]-[10]. Remember that we are considering a Taylor series expansion about a particular synchronized solution, not about the free-running oscillation. Thus, the analysis is general and can be applied for any input-power value. For convenience, we will define the following vector of increments:

$$\bar{X}(t) = \left[\Delta\phi_1(t)\ \Delta\phi_2(t)\ \Delta V_1(t)\ \Delta V_2(t)\right]^t \qquad (4)$$

Next, we translate system (3) to the frequency domain:

$$A(\Omega)\bar{X}(\Omega) = \bar{I}_N(\Omega) - \bar{\psi}(\Omega) \qquad (5)$$

where the matrix $A(\Omega)$ is given by:

$$A(\Omega) = \begin{bmatrix} Y^{1r}_{\phi_1} + j\Omega Y^{1r}_{\omega} & Y^{1r}_{\phi_2} & Y^{1r}_{V_1} & Y^{1r}_{V_2} \\ Y^{1i}_{\phi_1} + j\Omega Y^{1i}_{\omega} & Y^{1i}_{\phi_2} & Y^{1i}_{V_1} & Y^{1i}_{V_2} \\ Y^{2r}_{\phi_1} & Y^{2r}_{\phi_2} + j\Omega Y^{2r}_{\omega} & Y^{2r}_{V_1} & Y^{2r}_{V_2} \\ Y^{2i}_{\phi_1} & Y^{2i}_{\phi_2} + j\Omega Y^{2i}_{\omega} & Y^{2i}_{V_1} & Y^{2i}_{V_2} \end{bmatrix} \qquad (6)$$

and the vectors of noise sources correspond to:

$$\begin{aligned} \bar{I}_N(\Omega) &= \frac{1}{V_0}\left[I^r_{N1}(\Omega)\ I^i_{N1}(\Omega)\ I^r_{N2}(\Omega)\ I^i_{N2}(\Omega)\right]^t \\ \bar{\psi}(\Omega) &= j\Omega\psi(\Omega)\left[Y^{1r}_{\omega}\ Y^{1i}_{\omega}\ Y^{1r}_{\omega}\ Y^{1i}_{\omega}\right]^t \end{aligned} \qquad (7)$$

Due to the circuit symmetry, the following properties are fulfilled:

$$\begin{aligned} Y^1_{\phi_1} &= Y^2_{\phi 2} \equiv Y_\phi,\ Y^1_{\phi_2} = Y^2_{\phi_1} \equiv Y_{\phi c} \\ Y^1_{V_1} &= Y^2_{V_2} = Y_V,\ Y^1_{V_2} = Y^2_{V_1} = Y_{Vc} \end{aligned} \qquad (8)$$

which enable the simplification of matrix A. Next we invert the matrix A to solve for $\bar{X}(\Omega)$ and multiply by the adjoint $\bar{X}^t(\Omega)$. When performing these operations, it is considered that all the components of the noise vectors in (7) are uncorrelated stochastic processes and:

$$\left|I^r_{Ni}(\Omega)\right|^2 = \left|I^i_{Nj}(\Omega)\right|^2,\ i,j=1,2 \qquad (9)$$

The demonstration is too long to be included in the paper but it can be shown that some terms resulting from the described operations have negligible influence in the final expression, so the total phase noise power spectral density $\left|\Delta\phi_{Ti}(\Omega)\right|^2$ at each node i=1,2 of the push-push oscillator can be approached by:

$$\begin{aligned} \left|\Delta\phi_{Ti}(\Omega)\right|^2 &= \left|\Delta\phi_i(\Omega) + \psi(\Omega)\right|^2 \cong \\ &\cong \frac{\left|\bar{Y}_{VT} \times \bar{Y}_{\phi T}\right|^2 \left|\psi(\Omega)\right|^2 + 2\left|\bar{Y}_{VT}\right|^2 \dfrac{\left|\bar{I}_N\right|^2}{V_o^2}}{\left|\bar{Y}_{VT} \times \bar{Y}_{\phi T}\right|^2 + \left|\bar{Y}_{VT} \times \bar{Y}_{\omega}\right|^2 \Omega^2} \end{aligned} \qquad (10)$$

where $\times$ indicates the cross product and the vectors are composed by the real and imaginary parts of the corresponding complex magnitudes. The admittance derivatives in (10) are given by:

$$Y_{\phi T} = Y_\phi + Y_{\phi c},\ Y_{VT} = Y_V + Y_{Vc} \qquad (11)$$

Because there is a single phase reference in the circuit, the total phase derivative $Y_{\phi T}$ fulfills $Y_{\phi T} = -Y_{\phi g}$, that is, it is the opposite of the admittance-function derivative with respect to the phase of the input generator ϕ_g. The form of the approximate equation (10) is identical to the one obtained in [3] for the case of a single injection-locked oscillator (no push-push configuration). However, the phase and amplitude derivatives used in (10) are given by the expressions (11), that is, by the addition of the derivative with respect to the node voltage (phase) and the cross derivative with respect to the voltage (phase) at the other node. This is a significant result that will give rise to different phase-noise behavior in comparison with a single injection-locked oscillator.

The expression in (10) predicts two different frequency corners. The first corner occurs at the frequency at which the two terms in the numerator become equal:

$$\left|(\bar{Y}_V + \bar{Y}_{Vc}) \times (\bar{Y}_\phi + \bar{Y}_{\phi c})\right|^2 \left|\psi(\Omega)\right|^2 = 2\left|\bar{Y}_V + \bar{Y}_{Vc}\right|^2 \frac{\left|\bar{I}_N\right|^2}{V_o^2} \qquad (12)$$

The second corner frequency is obtained when the magnitude of the two terms in the denominator of (10) become equal. Expression (12) indicates that the 1st corner frequency will be higher for larger magnitude $\left|Y_\phi + Y_{\phi c}\right|$ and angle between $Y_{\phi T}, Y_{VT}$ close to 90º.

IV. Application to the Two Different Push-push Designs

The expression in (10) for the phase-noise spectrum has been applied to the two different push-push designs presented in Section II. The obtained results, shown in Fig. 3 can be compared with those obtained with the conversion matrix approach, with full HB simulations. To facilitate the comparison, the phase-noise spectrum is shown at the fundamental frequency in all cases. As can be seen, there is very good correspondence between the HB simulations and the semi-analytical approach in the two cases. For small offset frequencies, both oscillators copy the phase noise of the input generator, as predicted by (10). The original design has the first corner at an offset frequency of 20 kHz. From this point the optimized design exhibits a lower phase-noise spectral density, due to its higher first frequency corner.

The good accuracy of the semi-analytical formulation allows the use of this formulation to predict variations of the corner frequency versus any circuit parameter. Note that this expression of the corner frequency (12) can be introduced in the HB simulator, which it should be combined with an automatic calculation of the various derivatives at each synchronized steady-state solution. As an example, Fig. 4 compares the variation of the first corner frequency for the single oscillator circuit and the improved push-push design versus the input frequency ω_s. As can be seen, this corner frequency is always higher for the push-push oscillator, so a better phase-noise spectrum can be expected.

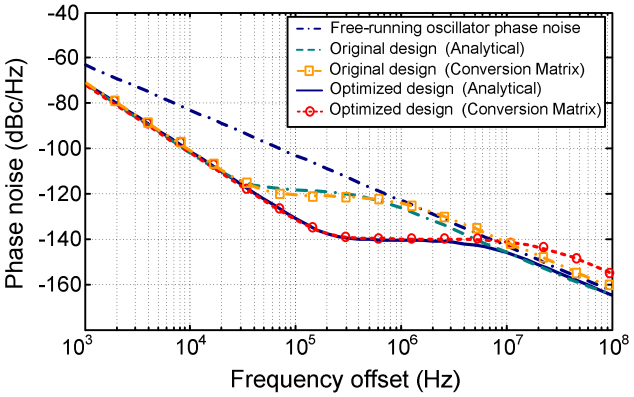

Fig. 3 Phase noise spectra for the original and optimized injection-locked push-push oscillators. Conversion matrix results are superimposed for comparison with the results of the analytical approach.

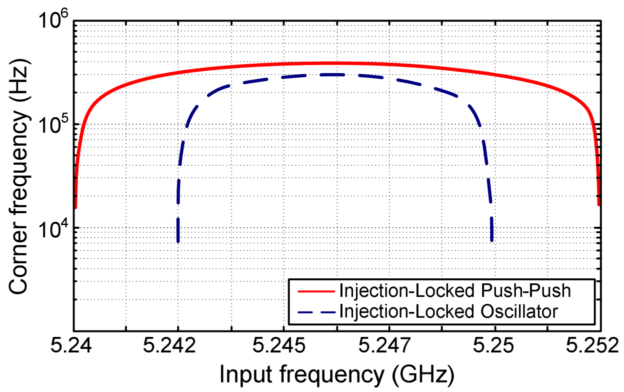

Fig. 4 Variation of the first corner frequency along the synchronization band for the single sub-oscillator and the optimized push-push oscillator.

For the above analyses a -30dB/dec characteristic has been assumed for the input generator. There are no qualitative changes for different input phase-noise spectra. For validation, the characteristic of an HP 83752A signal generator has been used in simulation. Fig. 5 shows the results of the analytical and conversion matrix approaches using this characteristic. The measured phase noise spectrum at the output of the circuit is also superimposed, showing very good agreement with the simulated results. To facilitate the analysis, the phase noise spectrum obtained with Eq. (10) is shown at the fundamental frequency (5.2 GHz), which explains the 6 dB difference compared with the measured spectrum at 10.4 GHz.

V. Conclusions

We have presented a semi-analytical approach for the in-depth understanding of the phase-noise spectrum of injection-locked push-push oscillators. The formulation enables an approximate prediction of the corner frequencies of the noise spectrum. It is possible to obtain the variation of these corner frequencies versus circuit parameters. We have applied the formulation to two different push-push designs with different locking bandwidth. The results have been successfully compared with harmonic-balance simulations and with measurements.

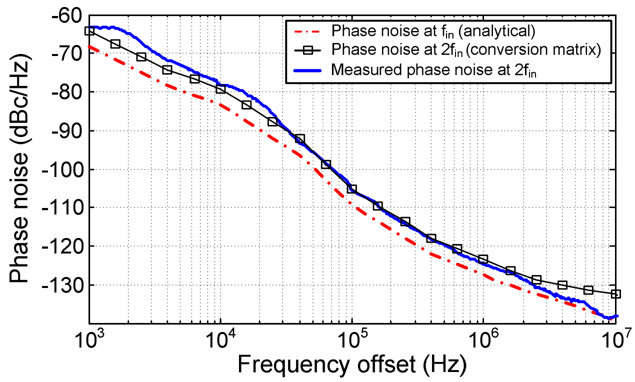

Fig. 5 Measured phase noise spectrum of the optimized injection-locked push-push oscillator. The results obtained with analytical approach (at f_{in}) and the conversion matrix (at $2f_{in}$) are also superimposed. The input phase-noise characteristic corresponds to an HP 83752A signal generator.

References

[1] F. X. Sinnesbichler, H. Geltinger and G. R. Olbrich, "A 38-GHz push-push oscillator based on 25-GHz f_T BJT's," IEEE Microwave Guided Wave Lett., vol. 9, pp. 151-153, Apr. 1999.

[2] F. Huang, Y. Chang, "A V-Band CMOS Injection-Locked Oscillator Using Fundamental Harmonic Injection", *IEEE Microwave and Wireless Components Letters*, vol. 17, no.12, pp. 882-884, Dec. 2007.

[3] F. Ramirez, M. Pontón, S. Sancho, A. Suárez, "Phase-Noise Analysis of Injection-Locked Oscillators and Analog Frequency Dividers", *IEEE Trans. Microwave Theory and Tech.*, vol. 56, no.2, pp. 393-407, Feb.2008.

[4] F. Ramírez, M. Pontón, S. Sancho, A. Suárez, "Stability analysis of oscillation modes in quadruple-push and Rucker's oscillators," *IEEE Trans. Microw. Theory Techn*., vol. 56, no. 11 (part 2), pp. 2648-2661, Nov., 2008.

[5] M. Pontón, E. Fernández, A. Suárez, F. Ramirez, "Harmonic-balance design and analysis of an injection-locked push-push oscillator", *Integrated Nonlinear Microwave and Millimetre-Wave Circuits*, 2008. Workshop on 24-25 Nov. 2008 pp. 53 – 56.

[6] E. Marazzi, V. Rizzoli, "The design of Linearizing Networks for High-Power Varactor-Tuned Frequency Modulators", *IEEE Trans. Microwave Theory and Tech.*, vol. 28, no. 7, July 1980, pp. 767 – 773

[7] J. Dominguez, S. Sancho, A. Suárez, "VCO Linearization Using Harmonic Balance," *IEEE MTT-S Int.,Microw. Symp. Digest, 2006.* Jun.2006 , pp. 864 – 867.

[8] F. Ramírez, E. de Cos, and A. Suárez, "Nonlinear analysis tools for the optimized design of harmonic-injection dividers," *IEEE Trans. Microw. Theory Techn.*, vol. 51, no. 6, pp. 1752-1762, Jun., 2003.

[9] A. Suárez, F. Ramírez, "Analysis of stabilization circuits for phase-noise reduction in microwave oscillators", *IEEE Trans. Microw. Theory Techn.*, vol. 53, no. 9, pp. 2743-2751, Sept., 2005.

[10] A. Suárez, Analysis and Design of Autonomous Microwave Circuits, Hoboken, New Jersey: Wiley - IEEE Press, 2009.